

EVALUATION OF THE VERTICAL DISPLACEMENT OF THE CIRCULAR FOUNDATION ON THE OVER-CONSOLIDATION GROUND IN PHU QUOC ISLAND, KIEN GIANG PROVINCE, VIET NAM

Thy Truc Doan*¹

¹Kien Giang University, 320 Route 61, Vinh Hoa Hiep, Chau Thanh Ward, Kien Giang Province, Viet Nam, e-mail: dtthy@vnkgu.edu.vn

*Corresponding Author

ABSTRACT

These research results were carried out comprehensively for the Circle foundation evaluation on the sand ground as results show the higher the pressure via the smaller the void ratio. On the other hand, the Particle size analysis test (PSAT) determines uneven particle size distribution at boreholes, so this shows 0.5% of affection to the vertical displacement of the circle foundation. However, the optimal loading capacity (q_u) obtains 20507.8 kN/m² and the permissible loading capacity (q_a) is 6851.86 kN/m², which has been considered the vertical displacement of the circle foundation 0.09m at 4.6m depth. Finally, comparisons of the vertical displacement between Terzaghi's evaluation with PLAXIS 2D software simulation have been done at a relatively small 0.05m value.

Keywords: Standard Penetration Test, Unconfined and Confined Compression Test, Particle size analysis Test, Vertical displacement, Terzaghi evaluation and PLAXIS 2D software.

1. INTRODUCTION

In recent years, the previous researches implemented an evaluation of settlement and loading capacity of the circle foundation on the sand ground behaviors with different methods and software simulations. To determine optimal loading capacity of the circular foundation, basic factors were considered particularly such as N_c , N_q , and N_γ and other affections to the radius, smooth, and rough foundation have also been calculated, whereas settlement of foundation didn't consideration (Amin and Jyant, 2017). Especially, the results also showed that the presence of oil in sand changes the mode of shear failure in the sand under the footing from local shear failure to the punching shear failure (Ahmed et al., 2019). FLAC numerical model indicates a significant decrease in the value of N_γ with an increase in the ratio of internal radius to the external radius of the ring. Results indicate that increasing the internal friction angle in expansion affects the loading capacity of the foundation that is different from the smooth and rough foundation (Benmebarek et al., 2012).

On the other hand, PLAXIS Introduction helps calculation of the circle foundation settlement on sand particularly with detailed descriptions for boundary conditions, materials, loading procedure, and nice color pictures, so the results can see and understand easily (Brinkgreve et al., 2014). This study shows how the existing solutions for the bearing pressure and footing structural resistance can be coupled to evaluate the impact of the soil-structure interaction (Cristiano and Lyesse, 2021). Factors N_c , N_q , N_γ affect foundation loading capacity under seismic conditions, and Terzaghi's formula to analyze the N_γ coefficient is also considered (Ernesto and Orazio, 2016).

In addition, the PLAXIS simulation presented a clear settlement of the circle foundation 5mm by supporting the pre-stress to the geotextile reinforcement 2% of the allowable tensile strength of the geotextile.

However, SPT (Standard Penetration Test) can't be mentioned (Julie et al., 2010). From the bearing capacity (η) of the overlying sand, the layer was evaluated through factors that include the layer thickness, the internal friction angle (ϕ), the surcharge pressure (q), undrained shear strength (c_u), unit weight (γ), radius of the foundation (b) and ratio of $c_u/\gamma b$. Result gave an increase of the layer thickness whereas value increase q and ratio of $c_u/\gamma b$, but the settlement of foundation didn't evaluation (Jyant and Manash, 2015).

On contrary, the finite element, upper bound plasticity, and stress field methods were employed to investigate the influence of inclined loading on the bearing capacity of a strip footing on a slope under undrained loading conditions. The shape of the vertical versus horizontal load interaction diagram depends only on the distance of the footing from the slope (normalized by the footing width) and the slope angle, provided that the failure mode is that of bearing capacity failure (Konstantinos, 2010). On the other hand, Using an elastic–perfectly plastic Mohr-Coulomb constitutive model for calculation of the effect of friction angle in expansion on the footing bearing capacity. rigorous LA bounds and MOC solutions regarding the shape factors for circular footings. The factors s_q and s_c always increase with increasing friction angle (ϕ) (Loukidis and Salgado, 2009).

However, a biaxial geo-grid and a geo-net are used for reinforcing the sand beds. Numerical results suggested that the geo-cell layer improves the bearing capacity by transferring the footing load to deeper soil layers and thus reduces the stresses and strains underneath the footing and completely arrests the surface have adjacent to the footing (Latha and Amit, 2009). Moreover, Method (UBFELA) described the relationship between the size of the cavity (D/B), depth (H/B), and the internal friction angle (u), so results show the ultimate bearing capacity of a strip footing influenced by an irregular underlying cavity in karst areas (Lianheng et al., 2021). Or a Mohr - Colum model and elastic - viscoelastic logarithm have been used for the soil behaviors. Results described the affection of parameters N_c , N_q , N_γ , and internal friction angle ($\phi < 250$) to the bearing capacity of the circle footing. But there is no mention of particle size consideration (Manoharan and Dasgupta, 1995).

Moreover, the slip-line method analysis of the classic Prandtl mechanism is not the plastic failure mechanism of the ultimate bearing capacity problem of perfectly smooth footings on weightless soil (Ming and Hong, 2019). And the (3D) three-dimension model simulation of the Finite Element method to evaluate the distribution of vertical stress under the footings in the soil medium with $\phi = 350$ and three cases of eccentricities: $e/D_0 = 0; 0.15; 0.3; 0.45$ when the footings are loaded under $q = 60$ kPa. The load eccentricity is applied at the right side of the footings and other factors N_c , N_q , N_γ are also considered in the loading process (Omid and Ehsan (2017). Two methods include FE (finite elements) and SOCP (second-order cone programming) analyzed the bearing capacity of a rigid strip footing on the clay ground, that gave in deformation of the shape related to the undrained shear strength ratio (c_{u1}/c_{u2}) and length/width of the foundation.

In other ways, it is necessary to consider the particle size test (Pingping et al., 2015). The rigid plastic finite element method (RPFEM) and The RPFEM method used for the ultimate bearing capacity, and results describe the distribution of contact stress along the footing base. The failure envelope in the plane of V/V_{ult} and M/BV_{ult} is further investigated under various conditions for the sandy and clayey soils M is the moment load induced by the eccentric vertical load (Quang et al., 2019). However, LAC simulations were used for the evaluation of the circle foundation with five different factors that include ratio N 's depending on settlement ratio and different rough conditions. Ratio N_c' increases as the ratio of D_f/D increases; the magnitude of the rough side is rather than the smooth side of the foundation...and so on (Sadok et al., 2017).

Finally, a new finite limit method was used to calculate the relationship between collapse load and parameters of the geometry changes, so results show particularly bearing capacity of the foundation. But

settlement and particle composition don't show clearly (Seyednima et al., 2019). The BRE470 method provides conservative results, which diverge from the FELA-calculated bearing capacities as the relative strength of the two layers q_b/q_t increases and is 70% lower than the thickness calculated via BRE470 (Sethy et al., 2019). And the National Standard System for Soils - Laboratory methods for determination of compaction characteristics help exact determination of experiments which include Standard Penetration Test, Unconfined and Confined Compression Test, Settlement (Viet, 2012).

From the above analysis, it is necessary to consider the effect of settlement (the vertical displacement) and loading capacity of the rigid foundation on the sand was implemented in the field and laboratory (Viet, 2012). Especially, under the assistance of PLAXIS 2D software simulation has also been implemented clearly to explain for settlement result of the circle foundation (Brinkgreve et al., 2014).

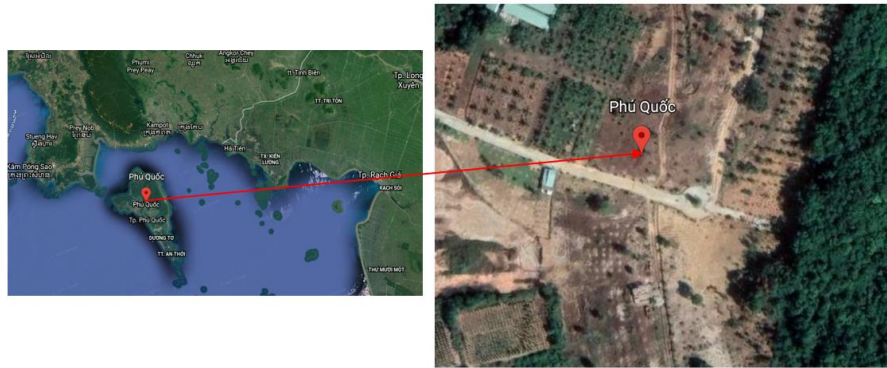


Figure 1: Location of the trial areas (Royal Bay, Phu Quoc Island, Kien Giang province, Viet Nam)

2. METHODOLOGY AND RESULTS

Field and experiment works were implemented by the Viet Nam Standard at pilot areas (Viet, 2012). The total of the drilling holes is 25 and every drilling hole includes 3 samples. The number of samples is 75 samples. The process was done carefully from the surveying stage, sample determination methods, sample covering, doing an experiment, calculation of results to simulate the PLAXIS 2D simulating software (Brinkgreve et al., 2014).

2.1 Field Experiment - The Standard Penetration Test (SPT), (Viet, 2012).

(Viet, 2012). the Standard Penetration Test (SPT) was implemented by the best tools and machines according to The National Standard System for Soils Laboratory methods for determination of compaction characteristics. Boreholes (HK) obtain 10.0m depth at three different locations from boreholes HK1 to HK25. After drilling and making holes that obtains requested depth. This works need to clean holes with bentonite liquid. Drilling of the soil layers 45cm thick and hammers have been dropped freely, which reached 7620mm height. Counting for the dropping hammers in each 30 cm segment. The number of piercing hammers (N-value) is a total of two times for counting, it is suitable to have a value of 30cm.

On other hand, if the sand layers with small to very small diameters and saturation, this means that the value of hammers $N > 15$ and results can be corrected by the formula 1 below:

$$N' = 15 + \frac{1}{2}(N - 15) \quad (1)$$

From the above results, we can determine the N-value according to the loading resistance capacity of many different depths. Results from Standard Penetration Test were shown in Figure 2, so soil characteristics have also been described particularly according to depth, thickness, and Standard penetration number (N-value) in table 1.

Table 1: The relationship between the standard load capacity and N-values (Viet, 2012)

Layer	Depth Z (m)	Thickness H (meter)	N-value N	Types of soils	Descriptions of states
1	1.5	From 1.5 to 3.5	From 7 to 12	Sand, semi- sand	Muld, mixed with organic impurities. Black – gray color, white – gray color.
1a	0.9	From 0.9 to 2.0	3	Sand mixed silt	Muld. White – gray color.
2	2.6	From 2.6 to 4.4	From 13 to 25	Medium coarse sand	Medium tightness. White – gray color and Yellow –brown color.
2a	4.4	From 4.4 to 9.3	From 13 to 21	Fine sand	Medium tightness. White – gray color and blue – gray color.

The Standard Penetration Test (SPT) has shown detailed values as this research is done at boreholes, which includes HK1 to HK 25 boreholes. At the borehole HK25, there is a big variation in values as compared with other boreholes, so results show remarkably. Figure 2 represented clearly that N-value changes with different depths. From boreholes HK1 to HK5, results are near the same, whereas, there is a strange change at HK3. On the other hand, with HK6 to HK10 boreholes, there are similar values. And two boreholes HK11 and HK12 varied particularly, whereas other boreholes HK13, HK14, and HK15 are a little similar. Lastly, boreholes HK16 and HK17 have clear variations as compared with HK18, HK19, and HK20 boreholes that are small changes.

2.2 Laboratory Experiment

2.2.1 Unconfined Compression Test (UCT) (Viet, 2012)

The laboratory experiment was done according to the Viet Nam Standard at the CIC GROUP in Viet Nam (Viet, 2012). Results describe particularly mechanical soil characteristics, layer thickness, states, and type of soils in table 2.

Table 2: Results of sand layer characteristics (Viet, 2012)

Layer	Unit specific weight γ_w (g/cm ³)	Floating unit weight γ_{dn} (g/cm ³)	Type of behavior	Yong's modulus E_1 (g/cm ²)	Poisson's ratio ν_{12} (g/cm ²)	Stiffness of soil E^* (g/cm ³)	Stiffness of soil increase with depth E^*_{inc} (g/cm ³)
2	1.839	0.96	Linear, isotropic	3.10^8	0.15	50000	5000

* Water unit weight $\gamma_n = 1\text{g/cm}^3$

Unconfined Compression Test (UCT) is one of the most special methods to determine the cohesive degree of soil, whereas evaluation of the void ratio according to the different load levels that measure settlements (vertical displacement). Moreover, Field and experimental works were implemented at the 25 boreholes with the 75 samples and depth increase from 0.0m to +2.0m and from +0.0m to 9.0m. The thickness of the pilot soil layer is from 2.2m to 4.6m (it means layer 2). Moreover, the relationship between different pressure levels (P) and void ratio (e) describes clearly the compressive soil in figure 3.

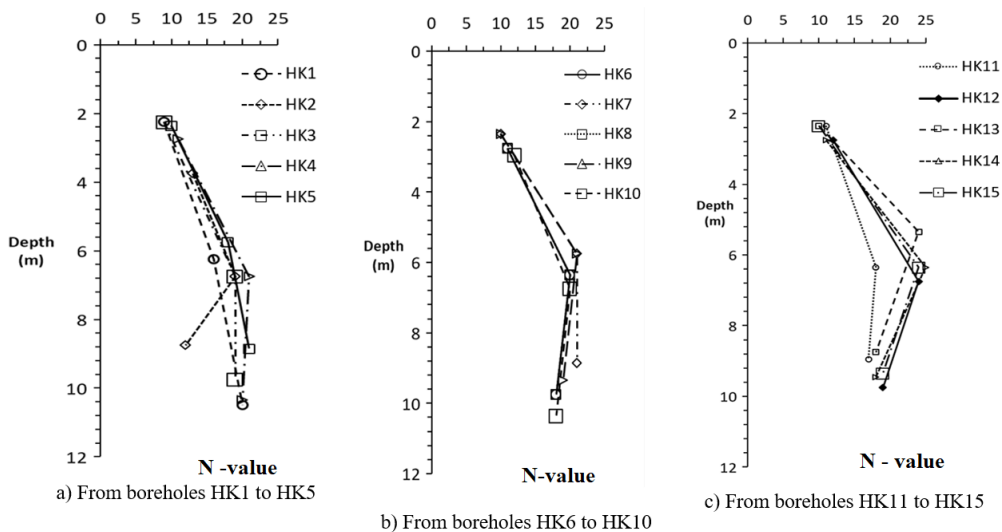
There are remarkable differences for the results of 11 samples in 25 boreholes such as borehole 2 (HK2); HK4; HK5; HK6; HK9; HK12, HK15; HK17; HK21; HK22, and HK23 boreholes, that is according to the different depths as 6.0m to 6.3m; 4.6m to 4.9m; 5.0m to 5.3m; 5.6m to 5.9m. The remaining boreholes have almost the same results include HK1; HK3; HK7; HK8, HK10; HK11; HK12; HK13; HK14; HK16; HK18; HK19; HK20, HK24, and HK25 boreholes, that is from 2.4m to 6.6m depths of the layer 2. Especially, void ratio of the borehole 12, 15, and 17 are most similar according to 6.0m to 6.3m; 5.60m to 5.9m; 5.0 to 5.3m depths, whereas remarkable differences show clearly between HK22 and HK23 boreholes at 5.60m to 5.9m and 3.0m to 3.3m.

From the above analysis, a remarkable decrease of the void ratio versus an increase of different loading levels, pore hole has broken, soil structure will be rearranged and deformation of the ground will occur faster, so this procedure results in the large vertical displacement of the foundation as loading. And consideration has been shown clearly at boreholes HK21, HK22, and HK23 boreholes.

2.2.2 Confined Compression Test (CCT) (Viet, 2012)

Confined Compression Test (CCT) has been implemented completely with 25 boreholes and 75 samples. On other hand, some particular differences for the results at boreholes 19 (HK19) with the sample 3 (S3) at 5.6m to 5.9m depth; HK20 with sample 3 (S3) at 8.6m to 8.9m depth; HK22 with sample 1 (S1) at 2.2m to 2.5m depth; and HK23 with sample 1 (S1) at 1.0m to 1.3m depth, that has seen clearly in figure 4. However, at 2.4m to 6.4m of layer 2, some boreholes and samples are no values so it is difficult to determine the degree of consolidation according to pressure levels.

From the result of figure 3, an increase of different pressure levels creates a decrease of void ratio, which cracks occur more and more on the soil surface, deformation of ground happen remarkably. Moreover, the resulting calculation was used in table 5, 6, and formula 18 to evaluation the vertical displacement of the foundation.



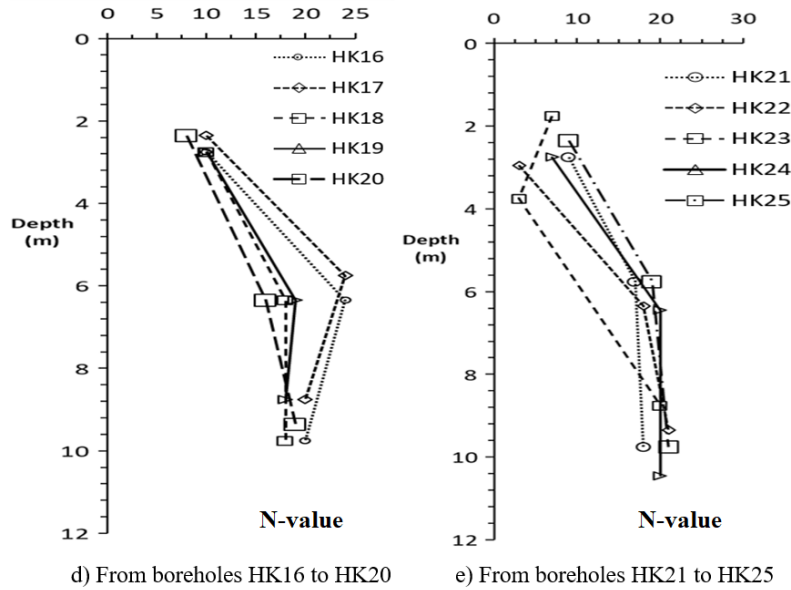


Figure 2: Results from Standard Penetration Test at different boreholes

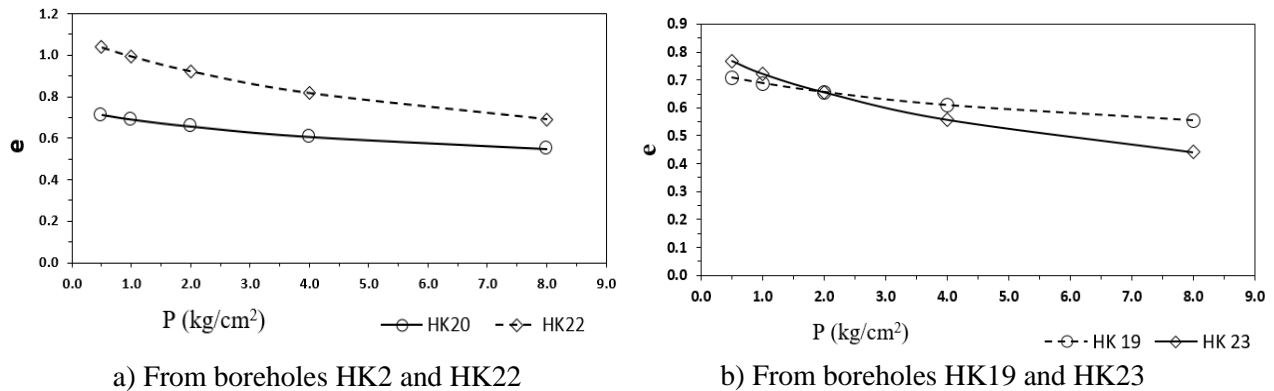


Figure 3: Results of the relationship between pressure (P) and void ratio (e)

2.2.3 Particle Size Analyzing Test (PSAT) (Viet, 2012)

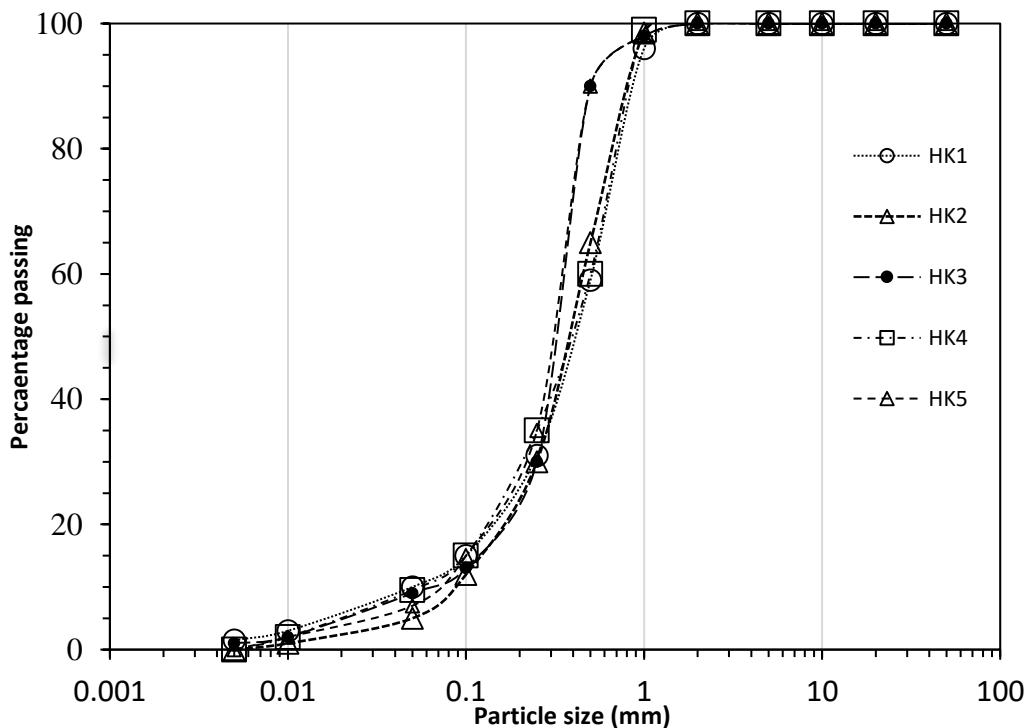
The particle size analysis test (PSAT) analyzed the relationship between the percentage of particle passing (%) and particle size (logarithm of values) at 15 boreholes with 75 samples and different depths. Variations of particle size described from 0.005mm to rather 100mm, but particle size from 50mm to 100mm at boreholes are similarity values. In contrast, the remarkable variations can see clearly from 0.005mm to 50mm particle sizes.

From figure 4a, the experiment has been done at boreholes HK1 to HK5 with different depths, that include 5.5m to 5.8m; 6.0m to 6.3m; 4.7m to 5.0m; 6.0m to 6.3m and 4.06m to 4.90 depths. It is easily to determine particle size diameters have less changed from 0.005mm; 0.01mm; 0.05mm and 0.1mm with maximum value 1.5%; 3%, 10% and 15%. Whereas, remarkable variations of the particle sizes have 0.25mm of the boreholes HK1 with 31%, HK2 with 30%, and HK5 with 35% of the percentage of particle passing. Moreover, it is rare to see particle size 0.5mm appears at HK5 with rather than 90% particle passing and

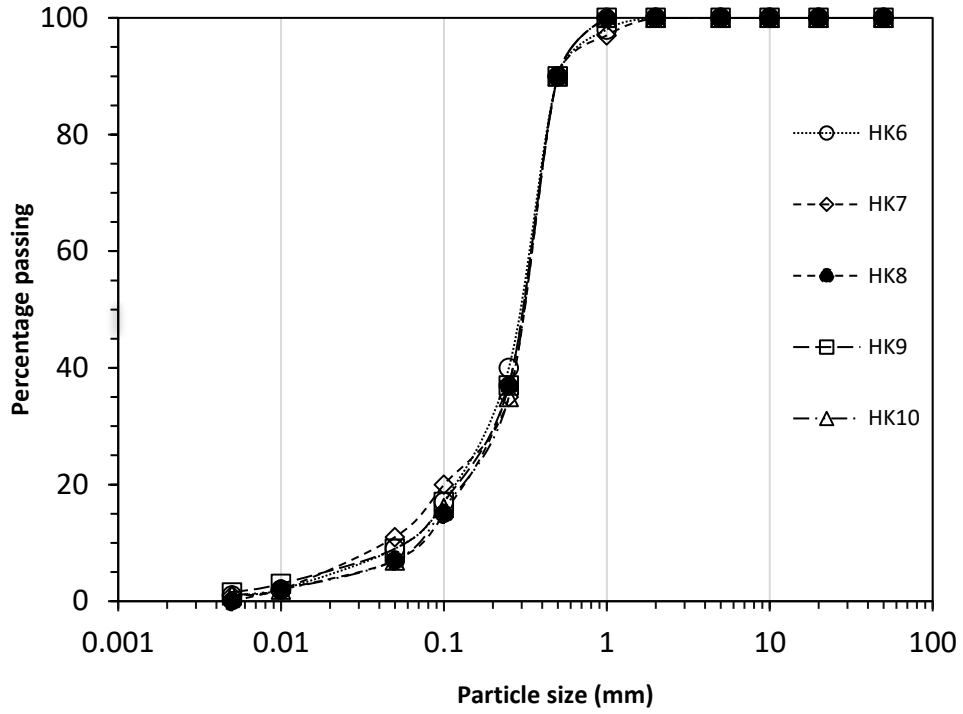
the remaining particle sizes only appear at HK5 with different passing percentage such as 1.0mm; 2.0mm; 5.0mm; 10.0mm; 20.0mm; 50.0mm with 96%; 98%; 99% and 100%. Whereas other boreholes are not.

From figure 4b, the experiment implemented at HK6 to HK10 with 6.0m to 6.3m; 6.0m to 5.3m; 5.6m to 5.9m; 5.0m to 5.30m and 6.0 to 6.3m depths. And there is a similarity as figure a, whereas analyzing the relationship between particle size diameters and percentage of particle passing. In additional, with particle sizes have 0.005mm diameters that occupy from 0% to 1.5% whereas with 0.01mm diameters appear from 2% to 3%. However, with 0.05mm diameters change clearly at HK6; HK7; HK8; HK9, and HK10 that are accounted for 15%; 16%; 17%, and 20%. On the other hand, with 0.1mm diameters distributed particularly of boreholes together, that means HK10 with 16%; HK9 with 17%; HK8 with 15%; HK7 with 20% and HK6 with 17%. Two boreholes (HK9 and HK10) have only occurred with 0.25mm diameter with 35% and 37% but it is clear that diameters from 0.5mm to 50mm only appear at borehole 10 with a difference of percentage of particle sizes 90%; 97%; 98% and 100%. And other boreholes can't show clearly as respectively.

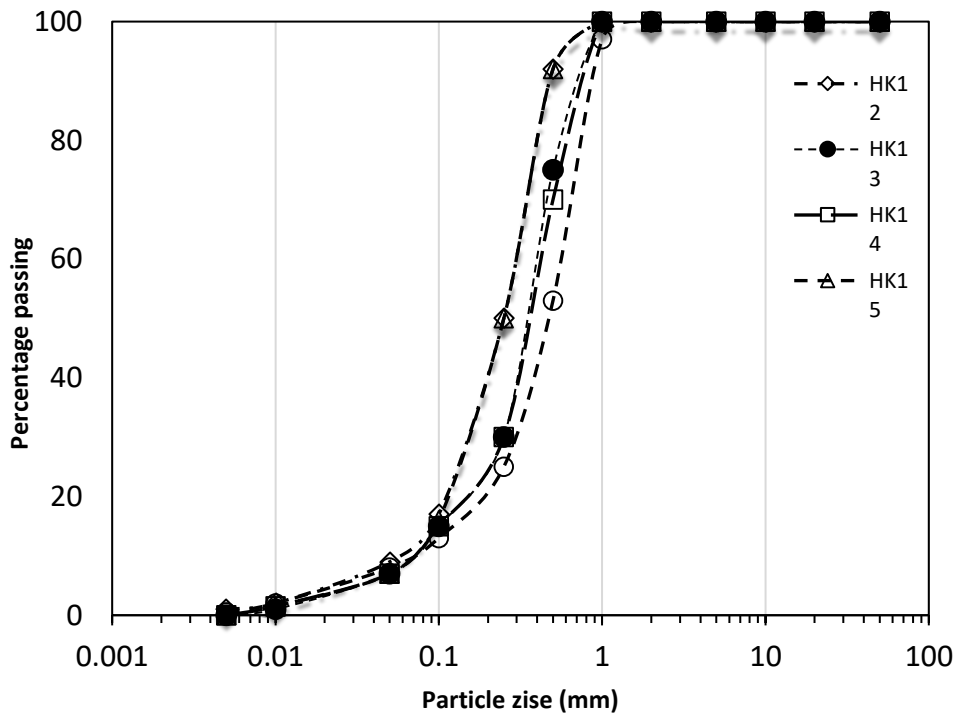
From figure 4c, experimental results have shown clearly at borehole HK11 to HK15 that describes 5.6m to 5.9m; 6.0m to 6.3m; 4.6m to 4.9m; 5.6 to 5.9m; 5.6m to 5.10m depths. There is a remarkable difference of boreholes together as a comparison between figures a, b, and c with 0.01mm diameter. From boreholes HK1 to HK10, the percentage of a particle passing clear changes and large differences whereas from HK11 to HK15, they have shown nearly and same values. On the contrary, no large variations of the percentage of a particle passing with 0.05mm and 0.1mm diameters are described clearly at HK1 to HK15. It is a similarity to conclude that figures b and c with 0.25mm diameter only appear at HK14 and HK15, whereas other boreholes can't show remarkably as respectively. Finally, from 0.5mm to 50mm diameters have shown clearly at borehole HK15 with 92% and 100%.



a) At boreholes (HK1, HK2, HK3, HK4, HK5)



b) At boreholes HK6, HK7, HK8, HK9 and HK10



c) At boreholes HK11, HK12, HK13, HK14 and HK15

Figure 4: Particle size distribution

From the above analysis, we can conclude that the relationship between particle sizes and percentage of particle passing has been shown clearly as determination values with 0.005mm to 0.1mm diameters, but there are large variations at boreholes HK4; HK5; HK9; HK10; HK14, and HK15 whereas other boreholes HK1; HK2; HK3; HK6; HK7; HK8; HK11; HK12 and HK13 can't appear values. On the other hand, diameter 0.005mm is account for 50% of total; 25% of 0.1mm diameter; 15% of 0.25mm; and 1% of 0.5mm diameter, and 9% of diameter (from 1.0mm to 50mm). So the percentage of the particle size distribution changes 0.5% of total particle volume that affect clearly to the vertical displacement (settlement) of the circle foundation on the sand ground.

2.2.4 Settlement (vertical displacement) of the sand ground

a) Theoretical basis of the optimal loading capacity

Settlement (vertical displacement) of the circular foundation on different grounds has already been researched in areas and countries in the world. Some researches were implemented with different methods by scientists (De Beer, Vesic, Hansen, Terzaghi, Meyerhof, Hanna, and so on), who showed clear results of the vertical displacement (settlement) of the shallow foundation on the different grounds. However, in recent years, some researchers have mentioned the relative factors, which include the foundation shape on the slip surface, vertical displacement, depth of foundation location, an inclination of the foundation, and so on. In this paper, we used the Meyerhof (1963), De Beer (1970), Hanna (1981), and Terzaghi (1973) methods to determine settlement (vertical displacement) of the circle foundation on the sand, that combine with PLAXIS 2D software simulation, so the results can be shown clearly at the different depths, whereas no any PLAXIS software simulation implemented on this ground during last time.

Optimal loading capacity of the ground under the circle foundation was implemented by De Beer (1970) that deepened on the real measurement of the foundations:

$$q_u = cN_cF_{cs}F_{cd}F_{ci} + qN_qF_{qs}F_{qd}F_{qi} + 0.5\gamma bN_\gamma F_{\gamma s}F_{\gamma d}F_{\gamma i} \quad (2)$$

Where factors affected to the foundation shapes F_{cs} , F_{qs} and $F_{\gamma s}$ were described particularly below:

$$F_{cs} = 1 + \left(\frac{b}{l}\right) \left(\frac{N_q}{N_c}\right) \quad (3)$$

$$F_{qs} = 1 + \left(\frac{b}{l}\right) t g \varphi \quad (4)$$

$$F_{\gamma s} = 1 - 0.4 \left(\frac{b}{l}\right) \quad (5)$$

Hansen (1970) suggested that factors affected the depth of the foundation location that considered for the ratio between the depth (D_f) and width (b) foundation.

$$\frac{D_f}{b} \leq 1; F_{cd} = 1 + 0.4 \left(\frac{D_f}{b}\right); F_{\gamma d} = 1 \quad (6)$$

Meyerhof (1963) and Hanna (1981) suggested that factors affected the inclination of the foundation as F_{ci} , F_{qi} , $F_{\gamma i}$.

$$F_{ci} = F_{qi} = \left(1 - \frac{\beta^0}{90^0}\right)^2 \quad (7)$$

$$F_{\gamma i} = \left(1 - \frac{\beta}{\varphi}\right)^2 \quad (8)$$

From the Field, Vesic (1973) corrected the loading capacity coefficients which included N_c , N_q , and N_γ values according to inclination angle (β) under foundation.

$$N_q = tg^2(45 + \frac{\varphi}{2} e^{\pi tg\varphi}) \quad (9)$$

$$N_c = (N_q - 1)cotg\varphi \quad (10)$$

$$N_\gamma = 2(N_q + 1)tg\varphi \quad (11)$$

Table 3: Results of the Optimal loading capacity (q_u) of the circle foundation (Terzaghi, 1956).

N (kN)	Φ (degree)	$\sigma_{bt} = \gamma D_f$ (kN/m ²)	N_q	N_γ	F_{qs}	$F_{\gamma s}$	F_{qd}	$F_{\gamma d}$	F_{ci}	$F_{\gamma i}$	q_u (kN/m ²)
150	26.34	18.39	19.173	13.196	3.63	0.6	0.34	1	0.61	0.06	20507.8

A circle foundation on the sandy ground with loading capacity (N) is 150kN, the inclination angle $\beta = 20^\circ$ according to the vertical dimension. The depth of the foundation location (D_f) is 1m (at layer 2). Because the groundwater level is at -10.0m so there is no affection of the groundwater level on foundation settlement. In this case, the calculation is considered as ignoring groundwater level. And foundation width D (diameter) obtains 3.0m with a safe coefficient (FS) is 3. The unit weight (γ) of the sand ground is 18.39 kN/m³ as a combination with internal friction angle (φ) is 26.34^o. Results show in table 4 below:

Table 4: Results of the relationship between (P_{gl}) and (P^{tc}) value (Terzaghi, 1956).

N^{tc} (Kg/cm ²)	$F = \Pi$ (D/2) ² (cm ²)	γ_{tb} (Kg/cm ²)	D_f (m)	γ (Kg/cm ²)	P_{gl} (Kg/cm ²)	P^{tc} (Kg/cm ²)
1.5	70650	0.22	100	0.1839	0.432	0.249

From the results above, it is necessary to conclude that the optimal loading capacity (q_u) is calculated quite exactly 20507.8 kN/m², so it is easy to determine the value of the permissible loading capacity (q_a) obtain 6851.86 kN/m² (with $q_a = \frac{q_u}{FS}$).

b) Settlement (vertical displacement)

Using the Unconfined Compressive Test (UCT) for determination of the settlement of the foundation at 2.4m to 4.6m depths and distance from 0.0m to the foundation bottom of layer 2 is 5.6m, where the depth of the foundation location (D_f) is 1.0m. Division the ground (Fig. 7) into small layers with a thickness of layers is 0.5m (from point 0 to point 5. Point 0 is the first point at the bottom, whereas four points under foundation points are 1, 2, 3, 4, and 5 according to 0.5m; 1.0m; 1.5m, 2.0m, 2.5m, and 3.0m depths. Terzaghi (1956) gave the assumption theory for the ground which worked as a linear elastic material. Moreover, pressure creates settlement at the foundation bottom (P_{gl}), which describes the increasing degree of the pressure by the building load, shown clearly in formula 12. On the other hand, standard pressure is located at the foundation bottom (P^{tc}), which shows the relationship between the standard building load on the area of the foundation (F) and the medium unit weight of the soil combined with the depth of the foundation location (D_f). The value (P^{tc}) is determined in formula 13.

$$P^{tc} = \frac{N^{tc}}{F} + \gamma_{tb} D_f \quad (12)$$

$$P_{gl} = P^{tc} - \gamma h \quad (13)$$

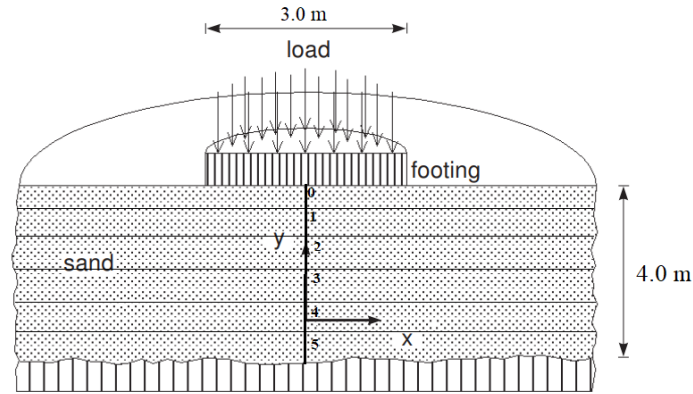


Figure 5: Division the sand layer under the foundation into small layers

Jaky (1958) gave in the formula to determine the horizontal pressure coefficient (K_0) of the soil (sand) at the stability state, which means the soil is at normal consolidation. And this theory is the most suitable for rambling soil and sand. Moreover, the relationship between the horizontal and vertical stress of the soil, which is at normal consolidation, is described through this K_0 value. However, in this paper, we used the K_0 value depending on the relationship between the ratio (z/b) and (L/b). Whereas L is the length of the foundation and with the circle foundation, value $b = L = D$ (with D is the diameter of the foundation). So it is easy to calculate, the vertical stress (σ_z) of points, which is at the central axis under the foundation bottom, go through the center of loading areas at depths z and the vertical stress (σ_z) is calculated by the combination between K_0 value and pressure creates settlement at the foundation bottom (P_{gl}),

$$K_0 = 1 - \sin \varphi \quad (14)$$

$$\sigma_z = K_0 P_{gl} \quad (15)$$

On the other hand, total stress is created by the unit weight of the soils (γ) according to the vertical dimension, which is at points with different distances from the ground surface to depth z , that is considered as the weight of the soil mass above is transmitted down the ground and the unit weight of the soils (γ) change with depth z .

$$\sigma_{bt} = \gamma z \quad (16)$$

Determination of the thickness of the compressive area H_n where sand ground receives the building load and it is easy to become deformation, so essential condition with the ground has deformation module (E) obtain value $E \geq 5 \text{ MPa}$ to ensure pressure create settlement (P_{gl}) is lesser than 0.2 their stress (σ_{bt}).

$$P_{gl} \leq 0.2 \sigma_{bt} \quad (17)$$

In addition, the total pressure at the foundation bottom (P_1) shows the medium stress value created by the relationship between the unit weight of the soil and depth. In contrast, the total value (P_2) describes the medium value of pressure which creates settlement. Both of these values are calculated for two layers together.

Finally, the results of the settlement of the circular foundation on the sand are implemented in formula 18 and table 6.

$$s = \frac{e_1 - e_2}{1 + e_1} (H) \quad (18)$$

Where H shows a total of the layer thickness (m); with $H = \sum_{i=1}^4 z_i$.
 e_1 and e_2 show the void ratio according to pressure P_1 and P_2
 s shows the settlement of the circular foundation (cm; m).

Table 5. Results of the relationship between void ratio (e) and pressure (P) at borehole HK5 (Terzaghi, 1956).

P (Kg/cm ²)	0.25	0.5	1.0	2.0	4.0	8.0
e	0.745	0.720	0.695	0.657	0.604	0.540

Table 6. Results of the settlement (vertical displacement)

Point	z (m)	z/b (cm)	K_0	P_{gl} (Kg/cm ²)	σ_{gl} (Kg/cm ²)	σ_{bt} (Kg/cm ²)	P_1 (Kg/cm ²)	P_2 (Kg/cm ²)	e_1	e_2
0	0.0	0.0	1	24.84	24.84	18.39	27.585	52.186	0.743	0.719
1	0.5	0.167	0.981	24.84	24.363	36.78	45.975	68.87	0.724	0.711
2	1.0	0.33	0.962	24.84	21.412	55.17	64.365	85.23	0.713	0.702
3	1.5	0.5	0.818	24.84	20.319	73.56	82.755	101.84	0.704	0.671
4	2.0	0.67	0.719	24.84	17.859	91.95	101.145	117.86	0.695	0.455
S (m) = 0.094										

c) Simulation by the PLAXIS 2D software (Brinkgreve et al., 2014)

- Boundary conditions

+ Project properties (Model properties)

Simulation of the PLAXIS 2D software by the finite element model. An appropriate boundary condition is applied at the bottom of the sand layer (Fig. 7). To enable any possible mechanism in the sand and to avoid any influence of the outer boundary, the model is extended in the horizontal direction to a total radius of 5.0m. The model keeps the default units in the Units that include “Length = m”; Force = kN; Time = day. A fixed gravity of 1.0 G, in the vertical direction downward (-z). The value of the acceleration of gravity is kept at a default value of 9.810 m/s². The unit weight of the water can be defined as 10 kN/m³. unit weight of water (γ_{water}) is 10 kN/m³. In the Contour group set the model dimensions to $x_{\min} = 0.0\text{m}$; $x_{\max} = 5.0\text{m}$; $y_{\min} = 0.0\text{m}$; $y_{\max} = 4.0\text{m}$. And the groundwater level is at -10.0m.

+ Soil stratigraphy

Boreholes are locations in the drawing area at which the information on the position of soil layers and the water table is given. In case of multiple boreholes are defined, PLAXIS 2D will automatically interpolate between the boreholes, and derive the position of the soil layers from the boreholes information. A borehole will be located at (x,y) = (0,0) and top boundary of the soil layer at z = 0; whereas the bottom boundary to z = -4.0m.

+ Material properties

By using the PLAXIS 2D software supporting, the settlement of the circular foundation on the sand at the loading time is simulated particularly during the active process of the foundation. The parameters appear in table 7 depending on the selected material model (in this case the Mohr-Coulomb model).

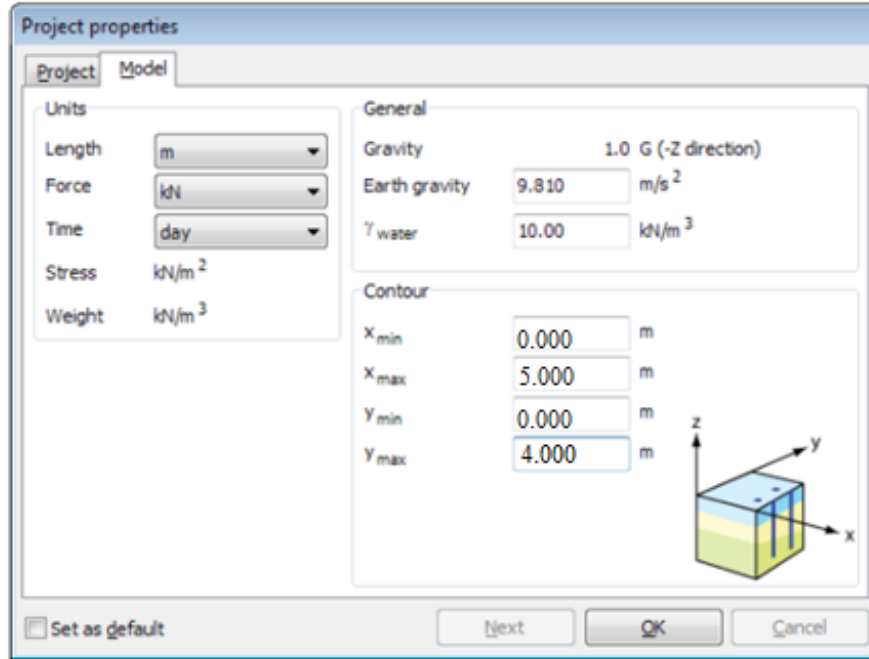


Figure 6: Project properties

Table 7. Material properties of the sand layer (Brinkgreve et al., 2014).

Parameter	Name	Value	Unit
General			
Material model	Model	Morh-Coulomb	-
Type of material behavior	Type	Drained	-
Soil unit weight above phreatic level	γ_{unsat}	15.36	kN/m ³
Soil unit weight below phreatic level	γ_{sat}	18.39	kN/m ³
Parameters			
Young's modulus (constant)	E'	$1.3 \cdot 10^4$	kN/m ²
Possion's ratio	ν'	0.3	-
Cohesion (constant)	c'_{ref}	1.0	kN/m ²
Friction angle	ϕ'	26.34	°
Dilatancy angle	ψ'	0.0	°
Initial			
K_0 determination	-	Automatic	-

+ Mesh generation

The software allows for a fully automatic mesh generation procedure, in which the geometry is divided into volume elements and compatible structure elements. The mesh generation takes full account of the position of the geometry entities in the geometry modal, so that the exact position of layers, loads, and structure is accounted for in the finite element mesh.

+ Performing calculation

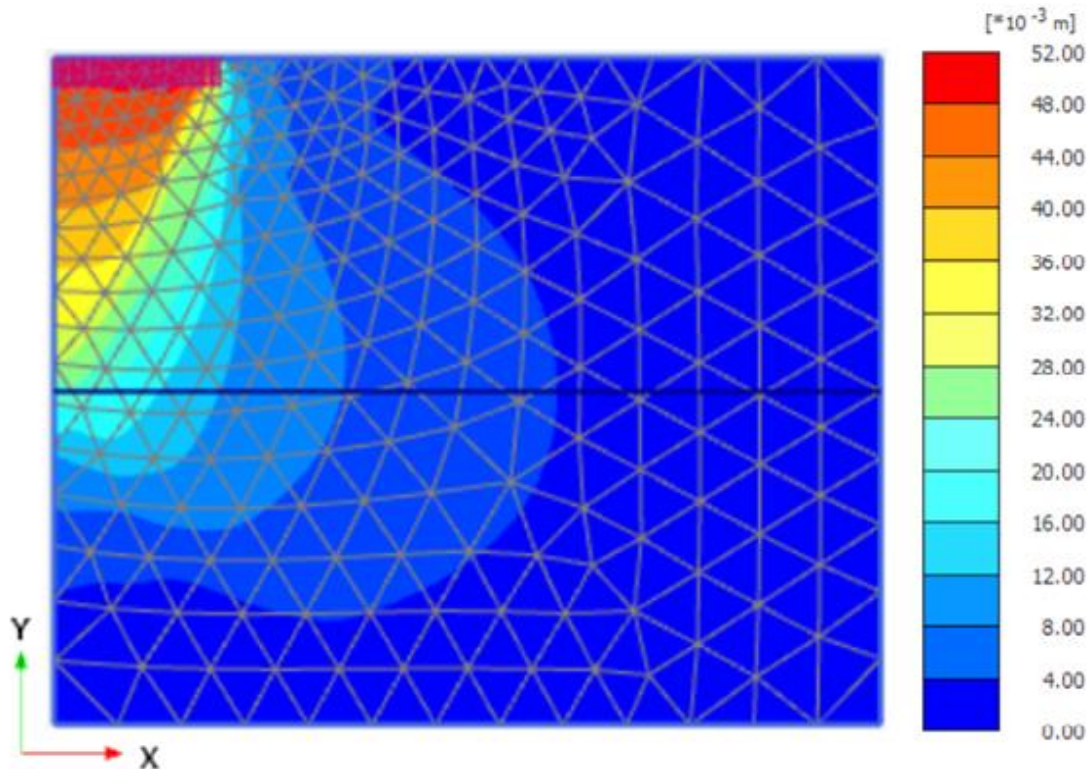
After finishing creating the mesh, two (2D) dimension models will be determined. In addition, during loading of the construction, two stages will be implemented and the K_0 value has always defaulted. Specify a uniform prescribed displacement in the vertical direction by assigning a value of -0.05 to $u_{y, start, ref}$,

signifying a downward displacement of 0.05m. At the first stage, it is necessary to create soils, initial geometry configuration, initial stress state, effective stress, pore pressures and state parameters, and so on. In contrast, at the second stage, we keep the same data as the first stage but there is a clear difference at this stage, we need to ignore the “geometry” factor and only the soil volumes are initially active. Both two processes don’t consider the affection of the groundwater levels.

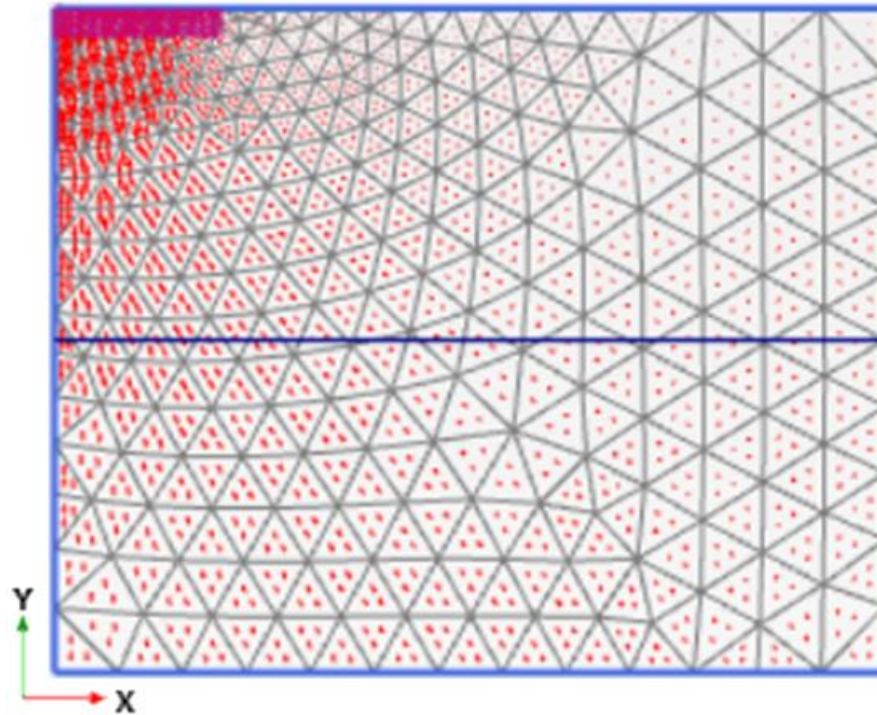
- Result calculations

From figure 7, it is easy to see that, the vertical displacement (settlement) of the circular foundation increase and extends according to the different depths, respectively. That is described with different colors from red, orange-red, orange, orange-yellow, yellow, green, a little blue, much blue, blue colors to dark blue color. Every color shows each depth according to the vertical displacement of the ground. Moreover, the minimum value of this displacement at 52×10^{-3} m depth with red color that is near the surface; In contrast, the maximum displacement value is shown clearly from 0.0m to 4.0×10^{-3} m depth.

On the other hand, with yellow and orange-yellow colors combine with displacement values from 28×10^{-3} m to 36×10^{-3} m, that has the little appearance and distribution uneven along deformation lengths. Especially, green color shows ground deformation overall of the length with 24×10^{-3} m depth. Lastly, the remaining colors include a little blue, much blue, blue colors that have deformed almost like green, so they are no big fluctuations. The above analysis proved that the closer to the surface, the greater the displacement, and decreases gradually with the greater depth. In addition, consideration of the stress distribution of the ground has also been shown particularly by the software support. With these results can consult civil and geology engineers or experts can estimate settlement of the ground before beginning construction and design procedures, so they can apply these results to minimize time, save costs for construction works in the future.



a) Total vertical displacements $|u|$. Maximum value = **0.05 m**



b) Maximum value = 9.568×10^{-15} kN/m²; Minimum value = -201.0 kN/m²

Fig 7. Result of the settlement (total vertical displacement)

3. DISCUSSIONS

The two-dimension (2D) dimension model of settlement (vertical displacement) of the sand under the circle foundation (rigid foundation) has been researched and evaluated remarkably at Royal Bay, Phu Quoc Island, Viet Nam. Results show carefully with remarkable values and especial combination and caparison of the PLAXIS 2D simulation and TERZAGHI formula crease best results as respectively.

Moreover, the Standard Penetration Test was implemented carefully to use and cover samples to avoid disturbing the soil sample that affected to mechanical characteristics of the soil. For this test, results show clearly the different loading resistance of the layers together. It is similar to determining value Particle Size Analysis Test (PSAT) was done at boreholes HK4, HK5, HK9, HK10, HK14, and HK15 boreholes, that with diameter changes from 0.25mm to 0.5m that is according to different depths. On other hand, the comparison between vertical displacement with TERZAGHI and PLAXIS 2D simulation is a little different. With the TERZAGHI method, the value obtains 0.09m but with PLAXIS 3D is 0.05m so the difference between the two methods isn't much. From there, the result of the vertical displacement of the circle foundation on the sandy ground with values in reliability as respectively.

4. CONCLUSIONS

From the above analysis, evaluation of the vertical displacement of the circular foundation on the sandy has more effective, so the paper's results consider affected factors such as optimal loading capacity, particle

size distribution change, deformation of ground depend on the relationship between void ratio and pressure, and software simulation at pilot areas.

Firstly, the Confined and Unconfined Compression Test was done at the boreholes from 1 to 25 with 75 experimental samples at depth change from 2.4m to 4.6m (from cote 0.0m) of layer 2. Especially, there are clearly different values at some boreholes HK19, HK20, HK 22, and HK23 of the confined compression test for the void ratio according to pressure levels.

Secondly, Particle Size Analyzing Test (PSAT) done successfully at the boreholes HK1 to HK10, percentage of particles passing clear changes and large differences whereas from HK11 to HK15. Diameter 0.005mm is account for 50% of total; 25% of 0.1mm diameter; 15% of 0.25mm; and 1% of 0.5mm diameter, and 9% of diameter (from 1.0mm to 50mm). So the percentage of the particle size distribution changes 0.5% of total particle volume, that affect clearly to the vertical displacement (settlement) of the circle foundation on the sand ground.

Thirdly, the optimal loading capacity (q_u) of the circle foundation on the sand ground obtain **20507.8** kN/m² and permissible loading capacity (q_a) is **6851.86** kN/m², so the loading capacity of the foundation is relatively good.

Finally, TERZAGHI evaluation and PLAXIS 2D simulation were used for the previous researches, but there is no concurrent combination of these two methods. Therefore, the results of the revised paper combination of these methods, whereas present a quite small difference (0.04m) for settlement of the circle foundation. The variation is 0.09m at 4.6m depth as compared with results simulation 0.05m, that is a small difference.

ACKNOWLEDGMENTS

1. Soil Mechanical Labor, Kien Giang CIC GROUP, in VIET NAM
2. Technology and Engineering Department, KIEN GIANG University, Viet Nam

REFERENCES

- B. Sadok, S. Insaf, B. Naima, *Journal of Rock Mechanics and Geotechnical Engineering*, **2**, pp.1-6 (2017).
- B. P. Sethy, C. R. Patra, B.M. Das. K. Sobhan, *Soils and Foundations*, **60**, pp. 13–27 (2020).
- C. Ernesto and C. Orazio, *Soil Dynamics and Earthquake Engineering*, **84**, pp. 204–223 (2016).
- D. Loukidis and R. Salgado, *Computers, and Geotechnics*, **36**, pp. 871–879 (2009).
- G. Latha and S. Amit, *Geotextiles and Geomembranes*, **27**, pp. 409–422 (2009).
- G. Konstantinos, *Computers and Geotechnics*, **37**, pp. 311–322 (2010).
- G. Cristiano and L. Lyasse, *Computers and Geotechnics* **134**, pp. 104-103, (2021).
- I. F. A. A. Ahmed, I. F Amjad, Y. F Mohammed, *Egyptian Journal of Petroleum*, **28**, pp. 281-288 (2019),
- K. Jyant and C. Manash, *Soils and Foundations*, **55**(5), pp. 1058–1068 (2015).
- K. Amin and K. Jayant, *Computers and Geotechnics*, **89**, pp. 33-42 (2017).
- L. Julie. L, K. Sanjay, and S. Nagaratnam, *Geotextiles and Geomembranes*, **28**, pp. 23–32 (2010).
- N. Manoharan, and S. P. Dasgupta, *Computers & Structures*, **54** (4), pp. 563-586 (1995).
- N. Viet, *The National Standard System for Soils - Laboratory methods for determination of compaction characteristics*, (Kien Giang CIC Group, Viet Nam, 2014), pp. 1-15.
- N. Quang, O. Satoru, I. Koichi, F. Yutaka, H. Takashi, *Soils and Foundations*, **59**, pp.1980–1991 (2019).
- R. B. J. Brinkgreve, W. M. Swolfs, S. Kumarswamy, *PLAXIS Introductory*, (Delft University of Technology, Netherlands, 2014), pp. 1-114.
- R. Pingping, L.Ying, and C. Jifei, *Computers and Geotechnics*, **69**, pp. 210–218 (2015).

- S. Benmebarek, M. S Ramadan, N. Benmebarek, L. Belounar, *Computers, and Geotechnics*, **44**, pp. 132–138 (2012).
- S. Omid and S. H. Ehsan, *Computers and Geotechnics*, **92**, pp. 169–178 (2017).
- S. E. Seyednima, J. Andrew, J. Abbo, K. George, *Computers, and Geotechnics*, **114**, pp. 103-101 (2019).
- X. P. Ming and X. P. Hong, *Soils and Foundations*, **59**, pp. 601–616 (2019).
- Z. Lianheng, H. Shan, Z. Zhonglin, Z. Rui, Z. Gaopeng and T. Z. Shi, *Soils and Foundations*, **61**, pp. 259–270 (2021).